Cancer Immunology, Immunotherapy (2020) 69:1751–1766
https://doi.org/10.1007/s00262-020-02575-y

ORIGINAL ARTICLE

In-depth characterization of the tumor microenvironment in central nervous system lymphoma reveals implications for immune-checkpoint therapy

Lukas Marcelis[1] · Asier Antoranz[1] · Anne-Marie Delsupehe[2] · Pauline Biesemans[1] · Julio Finalet Ferreiro[3] · Koen Debackere[4] · Peter Vandenberghe[5] · Gregor Verhoef[4,5] · Olivier Gheysens[6] · Giorgio Cattoretti[7,8] · Francesca Maria Bosisio[1,2] · Xavier Sagaert[1,2] · Daan Dierickx[4,5] · Thomas Tousseyn[1,2]

Received: 28 November 2019 / Accepted: 10 April 2020 / Published online: 25 April 2020

Abstract

Primary central nervous system lymphoma (PCNSL) is a rare type of non-Hodgkin lymphoma with an aggressive clinical course. To investigate the potential of immune-checkpoint therapy, we retrospectively studied the tumor microenvironment (TME) using high-plex immunohistochemistry in 22 PCNSL and compared to 7 secondary CNS lymphomas (SCNSL) and 7 "other" CNSL lymphomas with the presence of the Epstein–Barr virus and/or compromised immunity. The TME in PCNSL was predominantly composed of CD8+ cytotoxic T cells and CD163+ phagocytes. Despite molecular differences between PCNSL and SCNSL, the cellular composition and the functional spectrum of cytotoxic T cells were similar. But cytotoxic T cell activation was significantly influenced by pre-biopsy corticosteroids intake, tumor expression of PD-L1 and the presence of EBV. The presence of low numbers of CD8+ T cells and geographic-type necrosis each predicted inferior outcome in PCNSL. Both M1-like (CD68 + CD163^{low}) and M2-like (CD68 + CD163^{high}) phagocytes were identified, and an increased ratio of M1-like/M2-like phagocytes was associated with a better survival. PD-L1 was expressed in lymphoma cells in 28% of cases, while PD1 was expressed in only 0.4% of all CD8+ T cells. TIM-3, a marker for T cell exhaustion, was significantly more expressed in CD8^{pos}PD-1^{pos} T cells compared to CD8^{pos}PD-1^{neg} T cells, and a similar increased expression was observed in M2-like pro-tumoral phagocytes. In conclusion, the clinical impact of TME composition supports the use of immune-checkpoint therapies in PCNSL. Based on observed differences in immune-checkpoint expression, combinations that boost cytotoxic T cell activation (by blocking TIM-3 or TGFBR1) prior to the administration of PD-L1 inhibition could be of interest.

Keywords Immunotherapy · Primary central nervous system lymphoma · PCNSL · Tumor microenvironment · TME · TILS

Electronic supplementary material The online version of this article (https://doi.org/10.1007/s00262-020-02575-y) contains supplementary material, which is available to authorized users.

✉ Thomas Tousseyn
thomas.tousseyn@uzleuven.be

1 Translational Cell and Tissue Research Lab, Department of Imaging and Pathology, KU Leuven, Herestraat 49, 3000 Leuven, Belgium

2 Department of Pathology, University Hospitals, UZ Leuven, Leuven, Belgium

3 Center of Human Genetics, KU Leuven, Leuven, Belgium

4 Laboratory of Experimental Hematology, Department of Oncology, KU Leuven, Leuven, Belgium

5 Department of Hematology, University Hospitals, UZ Leuven, Leuven, Belgium

6 Department of Nuclear Medicine, University Hospitals, UZ Leuven, Leuven, Belgium

7 Department of Medicine and Surgery, Anatomic Pathology, Università degli Studi di Milano-Bicocca, Milan, Italy

8 Department of Pathology, Ospedale San Gerardo, ASST-Monza, Monza, Italy

Introduction

Primary central nervous system lymphoma (PCNSL) is defined by the 2017 revised WHO classification as primary diffuse large B cell lymphoma (DLBCL) of the CNS: an intracerebral or intra-ocular lymphoma excluding lymphoma of the dura, intravascular large B-cell lymphoma, lymphomas with evidence of systemic disease as well as immunodeficiency-related lymphomas [1]. PCNSL is categorized as a distinguishable entity from systemic DLBCL because of its unique clinical, histopathological and molecular features [2]. It is characterized by its rare occurrence, aggressive clinical course and poor prognosis which is worse compared to its non-CNS counterparts [3]. A subgroup of CNSL-DLBCL, particularly in immunocompromised patients with T cell immunodeficiency, are associated with Epstein–Barr virus (EBV) [4].

In the last decade, it became clear that besides the characteristics of the neoplastic cells, the composition of the tumor microenvironment (TME) has a significant prognostic importance in lymphomas, including PCNSL [5, 6]. The TME consists of all non-malignant elements surrounding the neoplastic cells including immune cells, stromal cells and non-cellular components. Studies have shown genetic and transcriptomic differences between PCNSL and DLBCL [2], but less is known of the TME in the CNS. The CNS is considered an immune privileged site, where immune cell access is strictly regulated by the blood–brain barrier.

Several retrospective studies in PCNSL using classical immunohistochemistry have observed a link between the TME and prognosis with a potential role for T cells and macrophages [3, 7–14] (Table 1). However, the focus has mainly been on perivascular areas without taking into account the T cells-infiltrating tumor bulk (TILs) or intra-tumoral heterogeneity [9, 12, 13], and the data on the prognostic effect of tumor-associated macrophages (TAMs) were contradictory [9, 12, 13].

PCNSL has a recurrent amplification of the 9p24.1 locus containing CD274 (encoding PDL1), PDCD1LG2 (encoding PD-L2) and JAK2 genes [15, 16]. This implies that patients with PCNSL could benefit from immune-checkpoint therapy, and phase 2 clinical trials with anti-PD-1 antibodies (NCT03255018, NCT02857426, NCT03798314) have been initiated. PD-L1 expression was insufficient as a biomarker to predict response to therapy [17], and until now, only a limited set of functional markers, such as PD-1 for cytotoxic

Table 1 Overview of published studies investigating the TME in PCNSL [3, 8–15, 22]

Study (references)	Year	DLBCL-PCNSL patients	Conclusions
Ponzoni et al. [7]	2007	96	Presence of reactive perivascular CD3+ T cell infiltrate is associated with ↑ OS. Presence of tumor necrosis has no prognostic significance
Kumari et al. [8]	2009	30	Reactive perivascular CD3+ T cell infiltrate shows no correlation with the different IELSG risk score groups. Tumor necrosis shows no correlation with the different IELSG risk score groups
Komohara et al. [9]	2011	43	The number of infiltrating CD68+, CD163+ and CD204+ TAMs has no prognostic significance.
He et al. [10]	2013	62	Presence of reactive perivascular CD3+ T cell infiltrate is associated with ↑ OS. Presence of aggregative perivascular tumor cells, stained with XBP1 and CD44, is associated with ↓ OS
Chang et al. [3]	2015	32 (+30 non-CNS DLBCL)	PCNSL has a ↓ OS in comparison with non-CNS DLBCL. PCNSL shows ↓ HLA-DR expression, ↓ number of S100+ dendritic cells, ↓ number of CD45RO+ effector or memory T cells in comparison with non-CNS DLBCL. For PCNSL patients, ↓ number of infiltrating granzyme B+ CTL correlated with ↓ OS
Four et al. [11]	2016	32	Expression of PD-1 in CTLs and PD-L1 in tumor cells was observed in higher rates compared with non-CNS DLBCL. PD-1 expression in CTLs correlated with PD-L1 expression in tumor cells. Presence of PD-1+ CTLs is associated with ↓ OS
Sasayama et al. [12]	2016	47	The number of infiltrating CD204+ TAMs shows no prognostic significance. ↑ number of CD68+ TAMs correlates with ↓ PFS on univariate analysis. Trends were observed for ↑ number of CD163+ TAMs and ↓ PFS on univariate analysis. The number of infiltrating CD68+ and CD163+ TAMs shows no prognostic significance on multivariate analysis
Cho et al. [13]	2017	76	↑ expression of CD68+ TAMs is associated with ↓ OS and ↓ PFS. FoxP3 expression in Tregs has no prognostic significance
Cho et al. [14]	2017	76	PD- 1 expression is associated with inferior OS
Miyasato et al. [20]	2018	5	PD-L1 and IDO1 were overexpressed by macrophage/microglia in PCNSL

TME tumor microenvironment, *PCNSL* primary central nervous system (CNS) lymphoma, *OS* overall survival, *IELSG* International Extranodal Lymphoma Study Group, *TAM* tumor-associated macrophage, *DLBCL* diffuse large B-cell lymphoma, *CTL* cytotoxic T cell, *PFS* progression-free survival, *Treg* regulatory T cell

T cells, were evaluated [11, 14]. Apart from the number of cytotoxic T cells, also the functional status of CD8+ T cells plays a role in response to immunotherapy [18]. Cytotoxic T cells can vary from naïve to stimulated 'active' cells and finally exhausted cells which are no longer functional [18]. This activation status is characterized by the expression of multiple markers such as OX40, CD69 for activation and LAG-3, TIM-3 for exhaustion [19]. Furthermore, little is known about the expression of immune checkpoints in macrophages/microglial cells except for limited data regarding PD-L1 [20]. The success of immune-checkpoint therapies in PCNSL remains anecdotal, and more insight in the TME is needed to determine the potential benefit for patients or a subset of patients with DLBCL located in the CNS [21].

To address the shortcomings of previous studies and address the new challenges raised by the development of immune-checkpoint therapies, we performed a digital, automated analysis of immunohistochemical stainings in both perivascular and central tumor areas on whole tissue slides in a cohort with available large excisional biopsies. Furthermore, we applied a novel high-plex staining technique (M.I.L.A.N.) [22, 23] on tissue microarrays (TMAs) to elucidate not only the phenotype of immune cells but also their functional status. Furthermore, we investigated microarray-based gene expression data.

Materials and methods

Patient selection

A list of biopsy reports over the last 20 years from the database at the Department of Pathology (University Hospitals UZ Leuven, Belgium) was generated based upon the search terms ("PNCSL" OR "CNS lymphoma") AND ("DLBCL" with CNS as biopsy site). Of the 126 cases that were withheld, histology was reviewed by two expert hematopathologists (T.T. and X.S.) and cases were classified according to the 2017 revised WHO criteria [1]. Cases not fitting the WHO criteria for primary DLBCL of the CNS, cases lacking sufficient formalin-fixed paraffin embedded (FFPE) material and biopsies with a surface smaller than 750,000 μm^2 (approximately 5 high power fields) were excluded. In total, 36 patients with biopsy confirmed DLBCL were retained. These cases were then subdivided in 3 groups: PCNSL ($n=22$), secondary CNS DLBCL (SCNSL) ($n=7$) and a rest group with EBV-positive CNS DLBCL or PCNSL arising in the context of immunodeficiency ($n=7$). PCNSL cases that did not meet initial inclusion criteria ($n=17$) due to insufficient material for full characterization and/or small size were used as a validation cohort for CD8 IHC-based survival analysis. This study was approved by the Ethical Committee of the University Hospitals Leuven (S-55498) and was conducted according to the Declaration of Helsinki.

Clinical data

The following clinical data were retrieved from the clinical files available at UZ Leuven: age, sex, immune status, International Extranodal Lymphoma Study Group (IELSG) prognostic score or International Prognostic Index (IPI), presence of extra-nodal or extra-CNS disease, first-line therapy and available follow-up data. Overall survival was calculated based on the date of biopsy confirmed diagnosis and status at last follow-up. The pre-biopsy therapeutic regiment was checked for intake of corticosteroids.

Immunohistochemistry and EBV-encoded RNA in situ hybridization

FFPE sections (3 µm) were used for all stainings. Since we wanted a minimum tissue surface of 750,000 μm^2, we included 20 excisional biopsies and 16 stereotactical needle biopsies. All antibodies were purchased from DAKO unless stated otherwise (supplemental table S1) and executed on an automated staining system (BOND RX or DAKO OMNIS). A threshold of 40%, and resp. 50% of malignant cells, was used to determine c-MYC and BCL2 positivity. All stainings required for diagnosis according to the WHO criteria were performed, and germinal center origin versus non-GC origin was determined according to the Hans algorithm (Supplemental fig. S1). The following TME stainings were performed on consecutive sections: CD4 and FOXP3, CD163 and PD-L1, CD8 and PD-1. The presence of EBV was determined by EBV-encoded RNA in situ hybridization (EBER) as previously reported [24].

Fluorescence in situ hybridization

Fluorescence in situ hybridization (FISH) for the 9p24.1 locus was performed in 5 cases with available frozen material and expression of CD274 (encoding PD-L1) in the neoplastic cells with an XL JAK2 (DC BA) 9p24 probe from Metasystems (Altlussheim, Germany) which encompasses the PD-L1 region of chromosome 9 as well. The FISH was performed according to the manufacturer's protocol. The number of positive signal dots per nucleus was evaluated for minimum 100 DAPI-positive cells. (Supplemental fig. S2). For all 11 C-MYC IHC positive cases, MYC FISH was performed with MYC [8q24, Vysis] break-apart probes and was evaluated as part of the routine diagnostic workflow. Additional FISH for BCL6 and BCL 2 was performed for those 2 cases with BCL6 [3q27, Vysis], and BCL2 [18q21, Vysis] break-apart probes.

Digital whole slide image analysis

All slides were scanned using the Philips ultrafast scanner 1.6, and automated analysis was performed using Qupath software v0.1.2 [25]. Firstly, as performed in previous studies, 6 perivascular areas were selected based on the presence of a perivascular rim of malignant cells or at a distance of max 100 µm from the outer edge of the vascular endothelium [7]. The size of the perivascular areas varied with blood vessel size, but contained an identifiable lumen at 200× magnification. Perivascular areas could be defined in 35/36 patients. Secondly, we analyzed 3 to 6 diffuse 'central' tumor areas based on biopsy size (totaling 600,000 or 1,200,000 μm^2), corresponding to a surface of more than 5 to 10 HPFs with a conventional light microscope. In cases with obvious intra-tumoral variation, 3 areas with a high cell counts and 3 with low cell counts were selected to capture this heterogeneity. In the 2 smallest biopsy samples, only 3 central areas could be evaluated and in the 9 cases with abundant geographic necrosis, viable tumor could only be evaluated in the perivascular areas. The analysis was repeated for 17 small PCNSL biopsies. Due to the small tissue size not enough clear blood vessels were present for perivascular analysis and the complete samples were analyzed. The percentage absolute nuclear count (ANC), corresponding to the percentage of positive cells over the total amount of nucleated cells present within each area, was calculated for CD8, PD-1, CD4, FOXP3 and CD163, similar to previous studies [26, 27]. The threshold for CD4-positivity was selected so that only strong staining lymphocytes were included and not the weak staining histiocytes (Supplemental fig. S3a-c). Cells co-expressing CD4 +/FOXP3+ were considered regulatory T cells (Tregs). CD163 IHC was evaluated using a threshold that only counted strongly positive cells to exclude false positive counting of neighboring cells due to a nearby dendrite.

Tissue micro-array generation and multiplex staining

Two tissue micro-arrays (TMAs) were generated using the 3DHistech TMA Grandmaster and 2-mm diameter needles. Cores were generated from 28/36 cases since in 8 cases with stereotactical biopsies the initial minimum amount of 3 cores per patient could not be obtained. Per patient 3–6 cores were selected based on sample size from random representative tumor areas to maximally capture potential heterogeneity, and in total, 109 cores were retrieved. Nineteen cores were excluded due to tissue damage and/or core detachment. In the final analysis, 90 cores consisting of 13 PCNSL, 4 secondary CNSL (SCNSL) and 5 "other" CNS DLBCL (4 EBV+ cases and one EBV-negative post-transplant CNS DLBCL) were used for analysis. Given that the total surface available for analysis of one 2-mm TMA core is tenfold that of a 0.6-mm-diameter core and 4 times the surfaced of a 1-mm-diameter TMA core as used in other PCNSL, cases with less than 3 remaining cores were not excluded [28]. Both TME slides were stained using multiple iterative labeling by antibody neo-deposition (M.I.L.A.N.) multiplex technique [22, 23] for 14 markers: CD163, CD3, CD68, CD8, FOXP3, HLA-DR, OX40, CD69, PD-1, LAG-3, TIM-3, PD-L1, S100AB and VISTA (supplemental table S2) and scanned with the Hamamatsu NanoZoomer S60 on 20× magnification. Images were processed using ImageJ and Cellprofiler.

Populations double positive for either CD8/PD-1 and CD68/CD163 were identified. A specific cell was defined positive for a marker if it contained a percentage of positive pixels over a threshold defined by Pareto optimality (Supplemental fig. S4). Al operations were done using the EBImage package (R statistical software). T cell activation was defined as described in Bosisio et al. [19]. CD69 and OX40 were selected as markers for T cell activation, while TIM-3 and LAG-3 were selected as markers for T cell exhaustion [19].

Gene expression profiling and pathway analysis

Micro-array-based gene expression data were prepared from 7 PCNSL samples as described by Morscio et al. [24] and performed with Affymetrix HG-U133 Plus 2.0 GeneChip (Affymetrix, HighWycombe, UK) according to manufacturers' recommendations.

Published DLBCL samples from the experiment described by Morscio et al. [24] ($n=8$) were included (Gene Expression Omnibus accession number: GSE38885) in the analysis as well as data from healthy brain tissue from different brain regions ($n=11$) analyzed on the identical microarray platform (GSE50161). A detailed overview of the included samples is available in table S3. Hierarchical clustering and inference analysis to identify differentially expressed genes were performed as previously described [24]. Differentially expressed genes compared to healthy brain tissue were filtered out using a minimal fold change of >1.5 and Benjamin–Hochberg corrected false discovery rate of <0.001. Criteria for significance in the final analysis of DLBCL versus PCNSL were Benjamin–Hochberg corrected false discovery rate of <0.05 and absolute fold change of >2.5. To identify significantly enriched gene networks, relevant pathways and biological functions in PCNSL versus DLBCL, the results of inference analysis were uploaded into the 'Ingenuity Pathway Analysis' application (IPA, www.ingenuity.com) as described previously [24]. Complete analysis results are available in supplemental data. Additionally, CIBERSORT analysis [29] was performed to deconvolute the tumor immune cell microenvironment based on the bulk microarray gene expression data and identify the proportion

of the 22 immune cell types present in the CIBERSORT LM22 panel [29].

Statistical analysis

Two patients had a very long (100 + months) survival compared to the other patients so their survival was trimmed to 36 months. Two cases were not used in any survival analysis since diagnosis was only confirmed during autopsy. For initial survival analysis, the strictly defined group of EBV-negative immunocompetent (IC) PCNSL ($n = 22$) was further divided based on the median % ANC of positive cells for different markers (CD4, FOXP3, CD163, CD8, PD-1) and defined areas (central, perivascular) creating each time a positive cell-high and positive cell-low group of equal size. For survival landscape analysis, continuous variables were dichotomized where the log-rank test yielded the most significant value. Given the relatively low number of patients, multivariate survival analysis was not performed. However, evaluation of the survival impact of each factor was performed independently, and for those that could predict survival, additional analysis in combination with CD8 scores was subsequently performed. Differences in proportions were tested using Chi square tests with Yates correction. The Shapiro–Wilk normality test was used to determine if data were normally distributed. Differences in means were tested using the Welch 2 sample *t* test for normal distributed data and the Mann–Whitney *U* test in the other cases comparing 2 groups. For comparisons with more than 2 groups, a Kruskal–Wallis rank sum test was used. Statistical determination of T cell activation/exhaustion status was performed as described by Bosisio et al. [19].

Results

General characteristics

The clinicopathological data of the final cohort of 36 patients are summarized in Table 2. Of those 36 patients, 22 were true primary CNS lymphoma (PCNSL) cases, 7 had either previous or concurrent nodal disease and were labeled as secondary CNSL (SCNSL), and 7 remaining were evaluated separately due to either presence of EBV ($n = 5$) or a presence of another factor with known effect on immune cells such as iatrogenic immunosuppression post-organ transplantation ($n = 2$).

Out of 36 cases (67%), 27 showed a diffuse growing lymphoma without dominant areas of necrosis and were labeled as "non-necrotizing" (Fig. 1a), while 33% (9/36) of cases showed a geographic type of necrosis, resulting in an angiocentric/perivascular presence of viable tumor and were labeled as "necrotizing" (Fig. 1b). Primary ($n = 22$) and secondary CNSL ($n = 7$) had a different prevalence of necrosis (23% vs. 0%), but this did not reach statistical significance in this cohort (Table 2). Necrosis was more prevalent in EBV+ (60% (3/5) compared to 19% (6/31) in EBV-negative cases ($p = 0.16$). The other CNS DLBCL group consisted of 5 EBV+ positive cases: 3 were EBV+ DLBCL, *not otherwise specified*, while the 2 others developed lymphoma while under immunosuppressive therapy (1 on systemic methotrexate (MTX) therapy for rheumatoid arthritis and 1 after a solid organ transplantation). The 2 EBV- cases in this group were EBV-negative post-transplant CNS lymphomas.

High-dose intravenous/intrathecal MTX was part of the initial therapy in 77% (17/22) of patients with PCNSL. Of the 5 other patients, 3 passed away before therapy and 2 received alternative chemotherapy regimens due to other clinical factors. Twelve patients received cortisone therapy prior to the biopsy, either as part of chronic maintenance therapy (6/36) or due to severe neurological symptoms (6/36).

BCL2 and C-MYC were expressed in 31% (11/36) and 72% (26/36) of cases, respectively. For the 11 cases overexpressing C-MYC by IHC, FISH analysis for MYC translocation could be interpreted in 10 cases. Two cases carried a t(8, 14)(q24;q32) IGH/MYC translocation: 1 PCNSL and 1 CNSL. Neither case had an additional BCL2 or BCL6 translocation. PD-L1 IHC revealed 2 patterns: PD-L1-negative tumors only staining phagocytes (in 26/36 or 72% of cases) and PD-L1-positive tumors, diffusely staining all malignant cells (in 10/36 or 28% of cases) (Fig. 1c). However, FISH, performed on the 5 PD-L1+ tumors with available frozen material (including 3 PCNSL and 2 SCNSL), did not reveal any amplifications of the 9p24.1 locus (Supplemental fig. S2).

There is a large inter- and intra-tumoral heterogeneity in the TME composition of PCNSL

Using whole tissue sections, a broad analysis was done of the TME in both central tumor bulk areas ($n = 27/36$, excluding the 'necrotizing' cases) and perivascular areas ($n = 36/36$).

In PNCSL ($n = 22$), CD163+ histiocytes and CD8+ T cells were the two major components of the TME (Fig. 1d-e) in the central tumor bulk with an average presence of 20.7% ANC and 9.4% ANC, respectively. Next, pairwise analysis of the central tumor bulk versus the perivascular tumor areas showed that both areas had a distinct TME composition. We observed an enrichment in CD8+ T cells in the perivascular region (18.3% ANC), compared to the central tumor bulk (9.4% ANC; $p = 0.001$). On the contrary, CD163 staining showed a slightly higher average histiocyte count in the tumor bulk (20.7% ANC) versus perivascular (17.6% ANC; $p = 0.8457$) (Fig. 1f). In the necrotizing cases, we noted a particular palisading

Table 2 Clinicopathological characteristics

	PCNSL ($n=22$)	Secondary-CNSL ($n=7$)	Other CNSL ($n=7$)	p value PCNSL versus SCNSL	p value PCNSL versus Other
Age (years)					
Mean [min–max]	68 [39–84]	49 [12–81]	66 [30–79]	0.013	0.98
Sex					
Male/female	15/7	3/4	2/5	0.45	0.158
Necrosis					
% (#)	23% (5/22)	0% (0/7)	57% (4/7)	0.417	0.213
EBV (EBER ISH)					
	0	0	5^{+}	/	/
Immunosuppressive/immunomodulatory therapy					
	0	0	4^{++}	/	/
Prognostic score (IELSG + IPI)	IELSG	IPI	IELSG ($n=4$) + IPI ($n=3$)		
Low risk (0–1)	4	1	1 + 0	NR	NR
Intermediate risk (2, 3)	11	6	2 + 1		
High risk (4)	1	0	1 + 2		
NA (incomplete data)	6	0	0 + 0		
3 year Overall Survival					
% (#)	9% (2/22)	29% (2/7)	20% (1/5[a])	0.501	1
High-dose MTX in first line					
Yes/no	17/5	5/2	2/5	1	0.057
Pre-biopsy corticosteroids					
Yes/no (NA)	7/13 (2)	1/6	4/3	0.581	0.562
Hans algorithm IHC					
GC/non-GC (NA)	0/19 (3)	2/4 (1)	1/4 (2)	0.078	0.463
c-myc IHC positive (> 40%[b])					
% (#)	36% (8/22)	29% (2/7)	14% (1/7)	1	0.53
Bcl2 IHC positive (> 50%[b])					
% (#)	82% (18/22)	57% (4/7)	86% (6/7)	0.411	1
PD-L1 IHC positive					
% (#)	23% (5/22)	29% (2/7)	43% (3/7)	1	0.581

PCNSL primary central nervous system lymphoma (CNSL), *EBV* Epstein–Barr virus, *EBER ISH* EBV-encoded RNA in situ hybridization, *IELSG* International Extranodal Lymphoma Study Group, *IPI* International Prognostic Index, *NR* not relevant, *MTX* methotrexate, *IHC* immunohistochemistry, *GC* germinal center

[a]Two patients were excluded because diagnosis was only confirmed at the time of autopsy

[b]Percentage of malignant cells used as threshold for positivity

arrangement of CD163+ histiocytes lining the viable tumor cells (Fig. 1g). There was a remarkable intratumoral TME heterogeneity, both for CD163+ histiocytes (with an average variation between highest and lowest analyzed area of 15.4%) and CD8+ T cells (average variation of 14.2%) (Supplemental table S3). CD4+ T cells were infrequent (average 1.8% ANC tumor bulk), and only rare Treg cells (CD4 +/FOXP3+; 0.65% ANC) or Tfh cells (CD4+/PD-1+; 0.64% ANC) were detected in the central tumor bulk. Only for CD4+ T cells, there was a perivascular enrichment observed (6.2% ANC vs. 1.8% ANC; $p=0.0003$). Perivascular enrichment for FoxP3+ cells was not observed ($p=0.13$). CD56+ natural killer cells were not observed.

Inter-tumoral TMA heterogeneity between patients was considerable with CD163+ histiocytes ranging from 5.8 to 36.5% ANC in the central tumor bulk. CD8+ T cells varied from 2.0 to 35.6% ANC. Since CD4+ T cells, PD-1+ T cells and FoxP3+ T cells were low in numbers, there was only a minor variation (0–9.6%, 0–2.2% and 0–2.9% ANC, respectively).

The pre-biopsy intake of corticosteroids (in 7/22 PCNSL cases) did not significantly affect the number of T cells or histiocytes. Neither was there a significant difference in

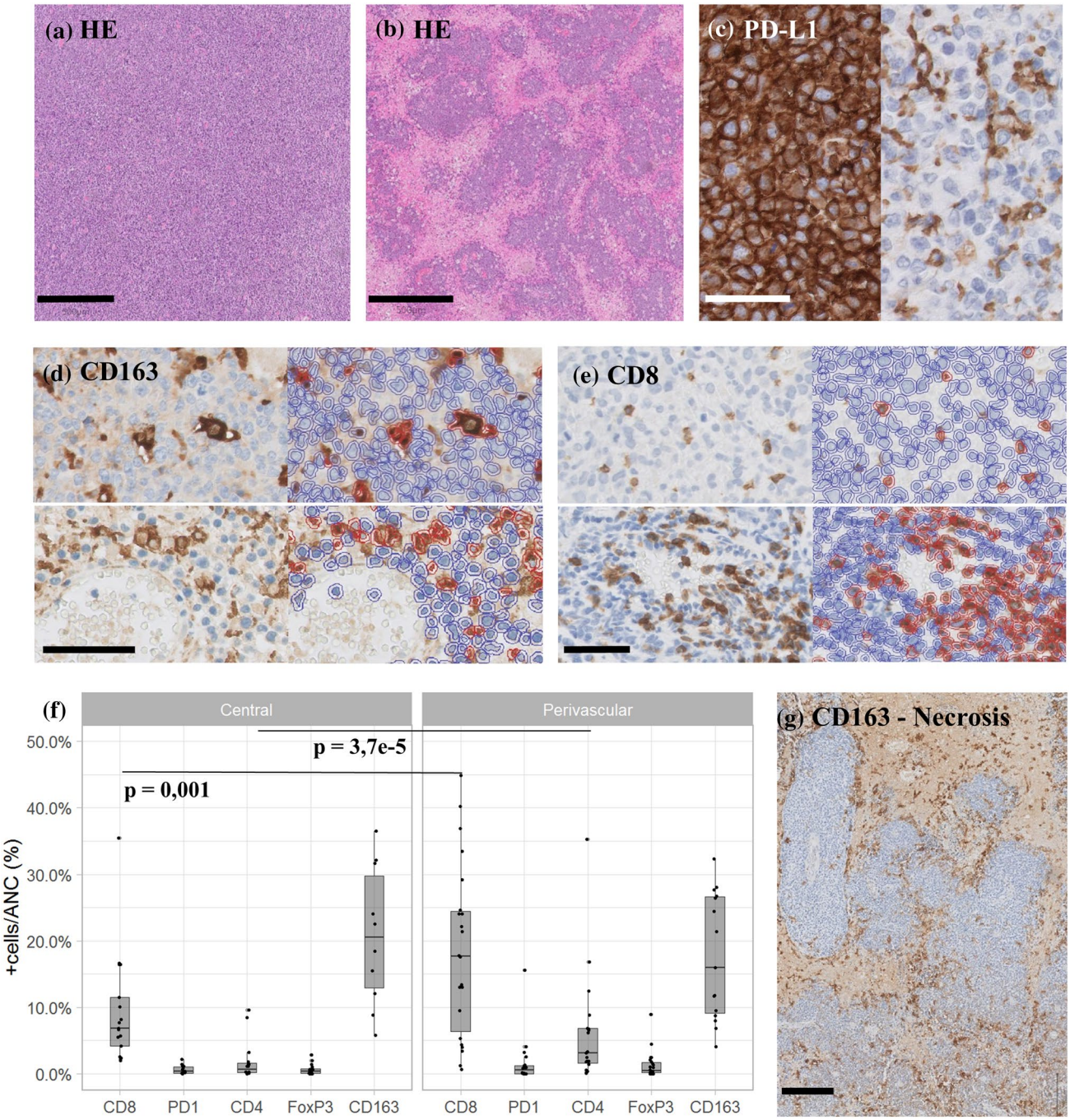

Fig. 1 Immunohistochemistry analysis. **a** Hematoxylin and eosin (HE) staining of a non-necrotizing case, scale bar 500 µm; **b** HE staining of a necrotizing PCNSL, scale bar 500 µm; **c** PD-L1 IHC illustrating staining of both neoplastic and phagocytic cells (left) versus staining of only phagocytes (tumor negative; right), scale bar 50 µm; **d** CD163 IHC (left) and Qupath overlay of positive/red and negative/blue cells (right) in both central tumor bulk (top panels) and perivascular (bottom panels), scale bar 100 µm; **e** CD8 IHC (left) and Qupath overlay of positive/red and negative/blue cells (right) in both central tumor bulk (top) and perivascular (bottom), scale bar 100 µm; **f** boxplots of average positive % ANC of IHC markers; **g** CD163 IHC of a necrotizing lymphoma biopsy with lining of the tumor by CD163+cells

number of T cells or histiocytes in non-necrotizing ($n=17$) versus necrotizing ($n=5$) PCNSL cases or in EBV+CNS-DLBCL ($n=5$) versus EBV-negative ($n=31$) CNS-DLBCL. However, when comparing PCNSL ($n=22$) versus SNCL ($n=7$), a significant difference in PD-1-positive cells was observed in the central tumor bulk ($p=0.02$) with an average

of 0.65% versus 0.13% ANC, and this difference remained true when comparing the average ratio of PD1 +/CD8+ cells ($p = 0.01$).

High CD8+ T cell presence, specifically in the central tumor bulk, is a robust predictor of better overall survival

Within the PCNSL cases ($n = 22$), we observed a significantly better survival in the CD8+ T cell-high group (divided based on the median), and this was valid both when counting cells in the perivascular ($p = 0.0014$) or central tumor bulk areas ($p = 0.013$) (Fig. 2a, b). The median number of CD8+ cells was 17.7% ANC (perivascular) and 6.8% ANC (central tumor bulk). Importantly, when excluding all patients who received corticosteroid therapy prior to the biopsy, only low CD8+ T cell counts in the central tumor bulk remained predictive for inferior outcome ($p = 0.0023$) but not perivascular ($p = 0.74$) (Supplemental fig. S5). Upon repeating the analysis for all CNS DLBCL ($n = 36$), the difference in survival remained significant for the central bulk areas ($p = 0.016$), but dropped just below significance level for the perivascular regions ($p = 0.09$). Survival curve landscape analysis was used to determine if the survival difference was robust when looking at all cases. The most sensitive cutoff for CD8+ T cells was 6.8% ANC ($p = 0.016$) in central tumor areas and 18% ANC for perivascular areas ($p = 0.035$) (Fig. 2e, f). Analysis was repeated in a second PCNSL cohort ($n = 17$) consisting of all cases not included initially due to small biopsy size (Supplemental table S4). A similar behavior was found for the CD8+ T cell cutoff of 6.8% ANC from the initial cohort (Fig. 2e) with again a trend toward better survival for the high-CD8 group ($p = 0.52$). No significant differences for any threshold were found for numbers of CD163+ histiocytes or CD4+ T cells.

Besides the composition of the TME, the presence of necrosis was also correlated with shorter survival in EBV-negative immunocompetent PCNSL ($p = 0.024$) (Fig. 2c) as well as the IELSG risk groups ($p = 0.015$) (Supplemental figure S6a). Of note is that necrotic cases were present in both previously defined CD8+ high and -low T cell groups without significant overrepresentation in one group ($p = 0.082$). When repeating the analysis only in the patients with necrotizing disease ($n = 9$), which already had a worse prognosis compared to patients with non-necrotizing disease, CD8+ T cell-high cases still had a better outcome ($p = 0.018$). All 2 'high-risk' patients, based on clinical prognostic score, had necrotic lymphoma and no central CD8 numbers could be determined. When comparing CD8 numbers within 'intermediate-risk' and 'low-risk' groups, high cytotoxic T cell numbers still showed better overall survival with a p-value of, respectively, $p = 0.15$ and $p = 0.075$ (Fig. S6b).

EBV positivity was associated with inferior outcome as well ($p = 0.02$) when evaluating all CNS-DLBCL ($n = 34$) although only 3 EBV-positive CNSLs were included in survival analysis (Fig. 2d). Two EBV-positive CNSL cases diagnosed during autopsy were not included. Interestingly, 2 of these 3 EBV+ CNSL were "non-necrotizing," and prognosis of these 2/27 non-necrotizing EBV+ cases was still significantly worse ($p = 0.0054$) compared to the EBV-negative, non-necrotizing cases.

PCSNL and SCNLS have similar patterns of T cell activation/exhaustion but multiple factors including the corticosteroid intake influence functional T cell status

To investigate the TME in more detail, multiplex staining analysis was performed on TMAs containing cores from 22/36 patients from the different groups (13 PCNSL, 4 SCNSL and 5 other CNSL of which 4 EBV +) in order to investigate the impact of these factors on the functional status of cytotoxic T cells in CNSL.

In the context of anti-PD-1 immunotherapy, we first determined CD8+ T cells and PD-1 co-expression in DAPI-positive objects (Fig. 3a) and the expression of other immune-regulatory proteins in these cells. Only 1578 (0.4%) of CD8+ T cells co-expressed PD-1. $CD8^{pos}PD1^{pos}$ cells expressed significant higher levels of T cell exhaustion marker TIM-3 on average compared to $CD8^{pos}PD1^{neg}$ cells (area under the ROC curve of 0.046 AUC) (Fig. 3b).

Since PD-1 is expressed immediately after T cell activation, further analysis of the functional status of cytotoxic T cells was done based on activation markers OX40 and CD69 and exhaustion markers LAG-3 and TIM-3 [19]. Expression of these markers was evaluated in each of the 40.041 identified CD8+ T cells using CD8-based cell segmentation (Fig. 3a). Different cores from the same patient showed a homogeneous activation status between the different cores except for patient no. 16 with 2 active and 3 exhausted TMA cores (Fig. 3c). PCNSL versus SCNSL did not reveal a difference in T cell functional status ($p = 0.44$). There were clear differences in average cytotoxic T cell activation/exhaustion status between patients who received corticosteroids prior to the biopsy versus those patients that did not ($p = 0.016$, PD-L1+versus PD-L1-disease ($p = 0.02$) and EBV+ versus EBV-CNSL ($p = 0.03$)). The presence of these factors was always associated with a shift toward T cell activation.

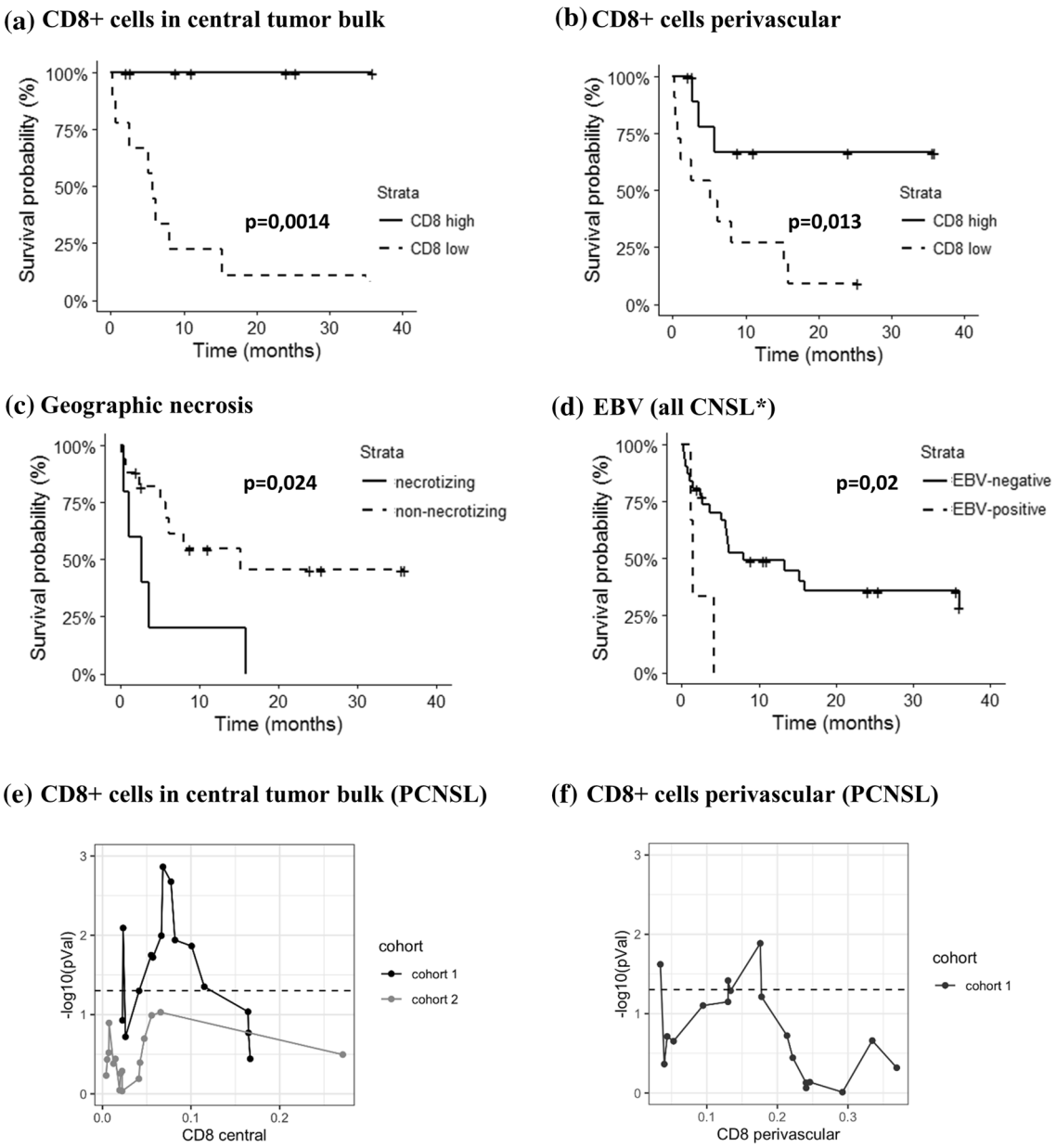

Fig. 2 Survival analysis. Kaplan–Meier survival plots for groups with high *versus* low number of CD8+cells in the perivascular (**a**) and the central (**b**) tumor bulk areas in PCNSL primary central nervous system lymphoma (PCNSL, $n=22$). Kaplan–Meier survival plots based on the presence or absence of necrosis in PCNSL (**c**) and EBV for all CNSL (**d**) excluding autopsy diagnosed cases ($n=34$); evolution of the Kaplan–Meier p value for all thresholds of CD8+cells in central tumor bulk (**e**) and perivascular (**f**) in PCNSL. The survival score is the −log10 of the p value; the relative rank is the position of the threshold in the list of all tested thresholds; the dashed line is the threshold for significance. Cohort 2 ($n=17$) is a validation cohort of small biopsies excluded from initial analysis. Abbreviations: NS, non-significant; S, significant

CNSL contains both M1-like and M2-like phagocytes with distinct immune-checkpoint expression profiles and inferior outcome for patients with low M1-like/M2-like ratio

As CD163+histiocytes were a major component of the TME in CNS-DLBCL, all phagocytic immune cells (microglial cells and tumor-associated macrophages) were therefore further characterized by high-plex analysis. Three subgroups of phagocytes were identified: a CD68+CD163^{low} (M1-like) group (181.451 cells, 17.2% of total), CD68+CD163^{high} (M2-like) group (77321 cells, 7.3% of total) and CD68-CD163^{high} group (32,787 cells, 3.1% of total) (Fig. 4a–c). These cell populations have a

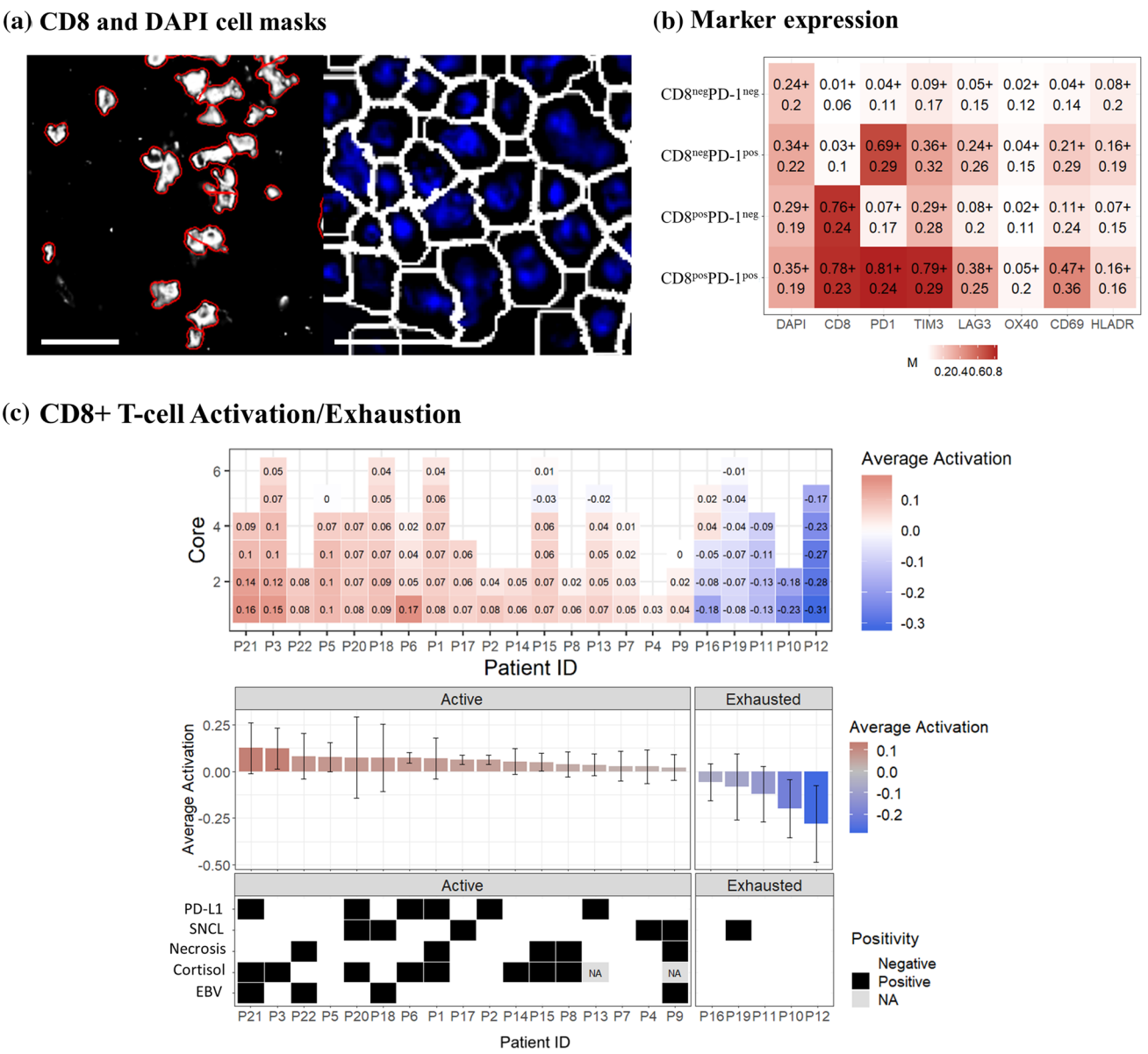

Fig. 3 Multiplex analysis of cytotoxic T cells. **a** CD8+ object identification image (Cellprofiler) used for subsequent activation/exhaustion analysis with identified objects outlined in red. Right panel: DAPI-based object identification (white outline) used to calculate CD8 and PD-1 double positive cell populations (R statistical software). Scale bar = 20 µm; **b** selected marker expression in the identified cell populations. The numbers in each square represent the average expression over all cells (± the standard deviation) for DAPI, CD8, PD-1, TIM-3, LAG-3, OX40, CD69 and HLA-DR; **c** average T cell activation status for each TMA core (square) of each patient (column) ranked from most active (left) to most exhausted (right) overall T cell status; **d** average T cell activation for each patient and correlation of this activation status to the PD-L1 expression on malignant cells (PD-L1), primary *versus* secondary CNS lymphoma (SNCL), presence or absence of geographic necrosis (Necr.) and relation to EBV (EBV), respectively

distinct expression profile of immune-checkpoint markers (Fig. 4d). Both CD68 + CD163^{low} (M1-like) phagocytes and CD68 + CD163^{high} (M2-like) phagocytes express PD-1 and PD-L1 in a subset of cells, while TIM-3 expression is more prominent in CD68 + CD163^{high} (M2) macrophages. VISTA was not convincingly expressed in any group.

No significant differences in average % of CD163+ phagocyte subgroups could be identified between PCNSL versus SCNL, EBV+ versus EBV-, necrotizing versus non-necrotizing or PD-L1-positive versus PD-L1-negative groups. However, a tendency for a lower amount of CD68 + CD163^{low} (M1-like) phagocytes was observed in patients with EBV+ (vs. EBV-; $p = 0.19$) and necrotizing (vs. non-necrotizing; $p = 0.2$) disease.

Interestingly, while no differences in outcome could be found based on the CD163+ histiocyte counts in IHC, an

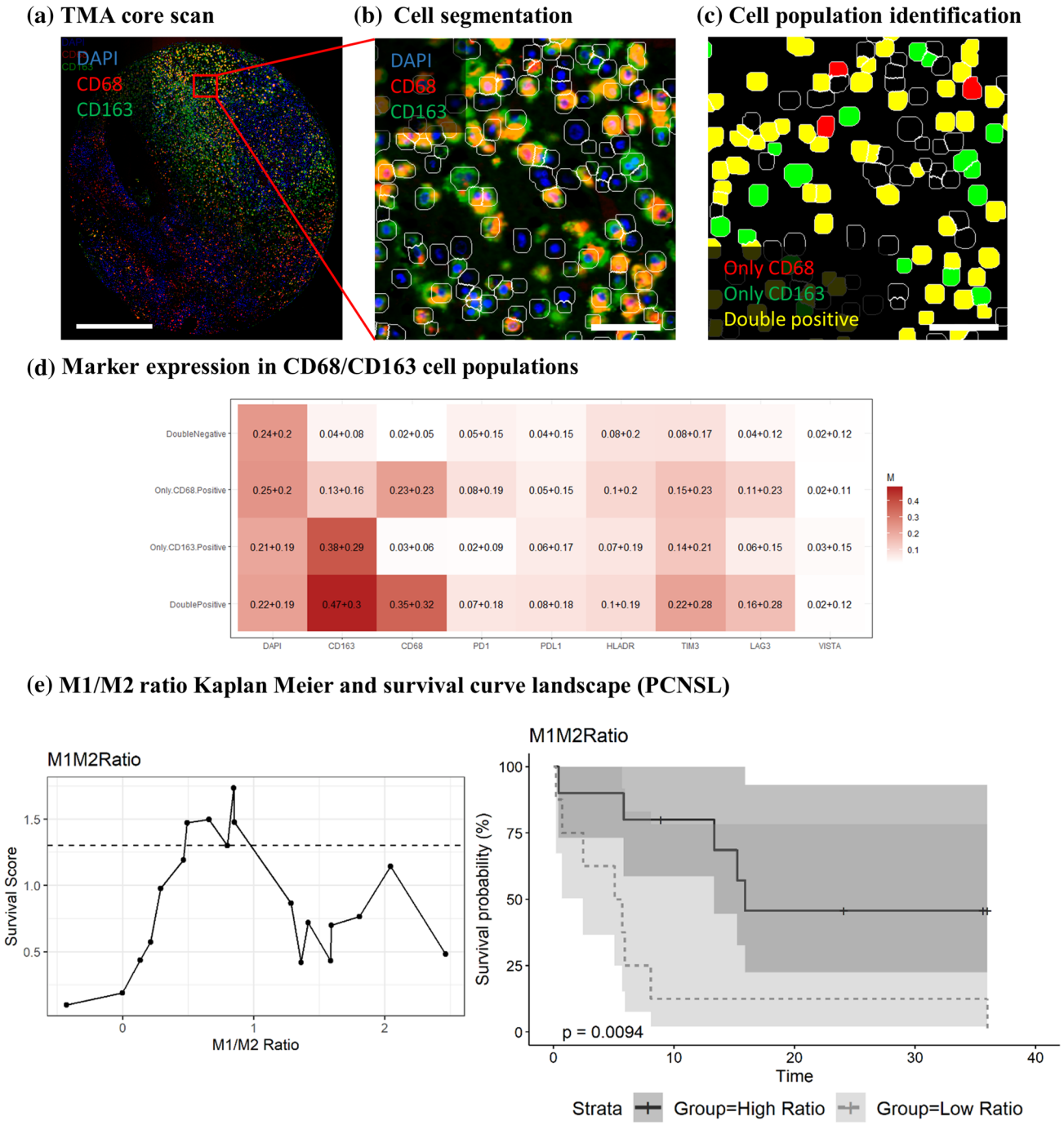

Fig. 4 Multiplex analysis of macrophages. **a** Processed immunofluorescence image of DAPI (blue), CD68 (red) and CD163 (green) used for subsequent analysis. Scale bar = 500 µm; **b** cell segmentation: magnification from TMA core region in (a) with additional DAPI cell segmentation mask (white outline). Scale bar = 50 µm; **c** cell population classification: CD68 only (red), CD163 only (green), CD68/CD163 double positive (yellow) and double negative (black). Scale bar = 50 µm; **d** selected marker expression in the identified cell populations. The numbers in each square represent the average expression over all cells (± the standard deviation) for DAPI CD163, CD68 PD-1, PD-L1, HLA-DR, TIM-3, LAG-3 and VISTA). The numbers in each square represent the average expression over all cells (± the standard deviation); **e** Kaplan–Meier survival curve (right) based upon the most significant ratio threshold (left). The survival score is the –log10 of the p value, and the x-axis contains the different possible M1/M2 ratios (left). The dashed line represents the threshold for significance. Abbreviations: NS, non-significant; S, significant

inferior outcome was observed in patients when dividing the patients into 2 groups of M1-like/M2-like phagocytes based on the median ratio which was also the most significant cut-off (ratio: 0.85; $p = 0.0094$; Fig. 4e).

Ingenuity pathway and CIBERSORT analysis reveal further evidence for immune modulation in PCNSL

Ingenuity pathway analysis (IPA) was performed for differentially expressed genes between 7 PCNSL cases and 11 DLBCL, and all cases were of non-germinal B-cell origin. Upstream regulator analysis was performed, and results were evaluated for factors with a potential impact on the TME. The top differentially expressed network compared to non-CNS DLBCL was "Hematological System Development and Function, Lymphoid Tissue Structure and Development, Tissue Morphology" DLBCL ($p = 10e{-}43$). The analysis revealed Transforming Growth Factor Beta Receptor 1 (TGFBR1) as a top upstream regulator with inhibited signaling in PCNSL compared to DLBCL (p value of overla$p = 5.45e{-}5$). The full IPA report is available as supplemental data (Supplementary material 2). CIBERSORT analysis was used instead to investigate the tumor immune microenvironment composition further based on the microarray gene bulk RNA expression data (Supplemental figure S7). CD8+ T cells were identified in PCNSL in slightly lower proportions as with IHC with an average 3.81% of total identified cells (vs. 6.8% in the central tumor bulk based on IHC), and this was lower but not significantly different from CD8+ T cell proportion in the DLBCL cases (average proportion = 10.09%; $p = 0.1$; p adjusted = 0.22). Interestingly, of the top 5 cases with most abundant M2-like macrophages, 4 were PCNSL. Higher abundance of M1/M2-ratio trended again toward better survival for these 7 PCNSL cases ($p = 0.2$) and performed equally to CD8+ T cell abundance ($p = 0.21$) (Supplemental figure S8). The most abundant immune cell type identified was memory B cell which most likely overlap the malignant cells given that all included PCNSL cased had a post-germinal center (non-GC) phenotype.

Discussion

In this study, we aimed to characterize the tumor microenvironment in CNS-DLBCL given the growing interest in immunotherapy for this aggressive disease. We performed a retrospective single-center histopathological analysis in 36 cases with large tissue surface available to capture heterogeneity and allow in-depth characterization. Next to 22 cases of PCNSL, we also included 7 cases of DLBCL metastasized to the CNS and 7 cases with other factors influencing the immune system of the patients such as iatrogenic immunosuppressive therapy and/or presence of EBV, factors potentially influencing the TME [30]. This together with evaluation of pre-biopsy intake of corticosteroids allowed us to investigate the effects of these factors on the TME.

The TME was shown to be heterogeneous in its distribution both between different areas in the bulk of the lymphoma of one patient as well as between the central tumor bulk and perivascular areas in one patient (intra-tumoral) and between patients (inter-tumoral). This heterogeneity was most outspoken for CD8+ cytotoxic T cells and CD163+ histiocytes, representing the two most prevalent cell types in CNSL. Previous studies focused primarily on the perivascular areas, which is the hypothetical point of entry of immune cells [31, 32] and showed little interest in the immune cells infiltrating the central tumor bulk. Specifically, the T cell distributions varied substantially with different amounts of CD4+ and CD8+ positive T cells between perivascular areas versus tumor bulk as previously suggested by some authors [13], but never objectified before. Interestingly, while both T cell subsets (CD8+ and CD4+) were enriched in perivascular areas, CD163+ cells on the contrary were slightly more present in the central tumor areas compared to perivascular, probably corresponding to activated CD163+ microglial cells.

We confirmed the positive impact on survival of the presence of high numbers of perivascular CD8+ cytotoxic T cells, as previously demonstrated [7, 8, 10], but without relying on manual counting or semiquantitative thresholds. These studies also heavily focused on evaluating the perivascular T cell component. In this cohort, we could demonstrate that when excluding all patients who received corticosteroids pre-biopsy, overall survival for patients with high numbers of CD8+ cytotoxic T cells remained significantly better in the central tumor bulk but not the perivascular area. Since central tumor bulk could only be evaluated in non-necrotizing lesions, the difference in survival was not confounded by the presence of necrosis which was an independent negative factor for survival in this cohort. The only 2 high-risk patients based on IELSG score both had necrotizing disease and were not included in central tumor bulk CD8 IHC analysis. When looking at central tumor bulk CD8+ T cells with the intermediate- and low-risk IELSG groups, respectively, high cytotoxic T cell numbers still rendered better overall survival. Survival landscape analysis showed that the effect of CD8+ T cells in the central tumor bulk is robust over different thresholds, but most significant with 6.8% ANC CD8+ T cells in central tumor bulk and 18% ANC CD8+ T cells in perivascular areas. Repeated analysis of central tumor bulk CD8+ T cells in a second cohort of 17 patients with PCNSL a similar behavior was observed. These were, however, small biopsies which could not be fully characterized. The small size might mean that those samples were less representative of the overall tumor which

could explain why significance was not reached. Numbers of tumor-infiltrating cytotoxic lymphocytes seem to have a clear and robust impact on clinical behavior strongly arguing in favor of immune-checkpoint therapies influencing these T cells. In order to use CD8 T cell numbers as an independent prognostic biomarker, larger multi-center studies are of course needed. The observed heterogeneity of CD8+ T cell infiltration in the central tumor bulk from nearly absent (1.9% ANC) to abundant (35.4% ANC) and impact on prognosis suggest, however, that further sub-selection of patients with PCNSL by evaluating if a PCNSL 'hot' or 'cold' might be necessary to achieve a significant response to immune checkpoint therapy in clinical trials. Furthermore, intratumoral heterogeneity raises the question on the representativity of small stereotactical biopsies as a tool to evaluate TME composition.

The composition of the TME, however, is not synonymous to the functional status of the immune cells present. This is especially relevant when considering current immune-checkpoint therapy aimed at rescuing exhausted cytotoxic T cells [33]. A more detailed investigation of cytotoxic T cells in CNSL lymphoma revealed that only 0.4% of all identified cytotoxic T cells expressed PD-1. However, the presence of PD-1-positive cells alone is not a valid biomarker for response to anti-PD-1 therapy in malignancies such as melanoma or lung cancer [34]. We therefore evaluated the functional status of the cytotoxic T cells in more detail. Analysis of the activation/exhaustion status of the cytotoxic T cells (based on the 4 functional markers OX40, CD69, LAG-3, TIM-3) revealed a wide spectrum of activation profiles between individual CD8+ T cells and between patients. The activation/exhaustion status of cytotoxic T cell depended upon corticosteroids intake, expression of PD-L1 by the neoplastic cells and presence of EBV. Due to the limited cohort size, multivariate analysis to determine the individual effect of these factors was not indicative (data not shown). Nevertheless, patients with the most exhausted cytotoxic T cells did not have any of these 3 factors present. Consideration of these factors affecting the functional status of T cell is required in the selection of patients for clinical trials with immunotherapy. For example, pre-immunotherapy corticosteroids to prevent cerebral edema will affect the functional status of the cytotoxic T cells and therefore most likely also the response to immunotherapy.

No amplification of the 9p24.1 gene locus containing PD-L1 was detected in for the 5 cases with available frozen material; multiple other mechanisms can explain PD-L1 expression in these non-Hodgkin lymphomas. EBV directly influences PD-L1 expression through its viral protein LMP1 and indirectly through activation by inflammatory cytokines [35]. PD-L1 expression through the activation of the JAK2/STAT3 pathway can also occur through molecular alterations such as loss of SOCS-1 inhibition or via inflammatory cytokines such as IL10. The MYD88 L256P mutation can potentially activate JAK/STAT signaling, and PD-L1 expression is described as an early mutational event in PCNSL [35, 36].

We also investigated the expression of other potential immunotherapy targets, like LAG-3 and TIM-3 in T cells, for which novel therapeutics are currently under development [33]. TIM-3 was strongly expressed in both $CD8^{pos}PD\text{-}1^{pos}$ and $CD8^{pos}PD\text{-}1^{neg}$ T cells giving it potential synergy with anti-PD1 therapy. Significant enrichment of TIM-3 (exhaustion) in $CD8^{pos}PD\text{-}1^{pos}$ cells together with higher expression of CD69 compared to $CD8^{pos}PD\text{-}1^{neg}$ T cells is compatible with the expression of PD-1 already early after activation until exhaustion [37]. Insights in the mechanisms of T cell activation and exhaustion are still developing quickly. CD69 is a type II glycoprotein known to regulate inflammation through T cell migration and retention in tissues. It is, however, not just a marker of T cell activation, but also initiates T cell exhaustion through first $PD\text{-}1^{high}TIM3-$ 'weakly exhausted' T cells to $PD\text{-}1^{high}TIM3+$ 'extremely exhausted T cells' [38].

The other major components of the TME were CD163+ histiocytes. In contrast to Hodgkin lymphoma, where abundant CD163+ histiocytes are considered a predictor of worse prognosis [39], we could not find significant differences in outcome for any threshold for CD163+ counts based on immunohistochemistry. Similar results were observed in previous studies, both in PCNSL or all-CNSL [9, 12, 13]. Still their potential relevance in response to immunotherapy [40] warranted further investigation. Using multiplex image analysis, we identified different CD163+ phagocyte populations: $CD68+CD163^{low}$ (M1-like), $CD68+CD163^{high}$ (M2-like). Although each independently showed no correlation with outcome, patients with a lower ratio of M1-like/M2-like phagocytes showed an inferior outcome. This implies that the combination of more M2-like pro-tumoral phagocytes and less M1 anti-tumoral phagocytes together does have an impact on the clinical behavior in PCNSL. The detection of different phagocyte subtypes highlights the complexity of identifying immune cell subsets, the danger of identifying more complex immune cell types based on a single marker and the need for multiplex in TME evaluation. The expression of immune-checkpoint proteins in phagocytes and their impact on immunotherapy are not well characterized, but the observed increased expression of TIM-3 in the pro-tumoral M2-like phagocytes in combination with the exhausted cytotoxic T cells is of potential interest for anti-TIM-3 immunotherapy [33, 41].

In summary, TIM-3, a marker for T cell exhaustion, was expressed in both $CD8^{pos}PD\text{-}1^{pos}$ T cells and $CD8^{pos}PD\text{-}1^{neg}$ T cells and had an increased expression in M2-like pro-tumoral phagocytes versus M1-like anti-tumoral phagocytes.

Together with an observed impact of M1/M2 ratio on overall survival makers, it is an interesting target for immunotherapy in CNS-DLBCL either alone or more likely in combination with anti-PD-1 therapy.

Microarray-based gene expression studies were performed on 7 cases of PCNSL and compared to previously published non-germinal center DLBCL cases [24]. Ingenuity Pathway Analysis was done comparing PCNSL versus nodal DLBLC after removing differences caused by the presence of CNS-tissue. TGF-β receptor 1 (TGFBR1) signaling-related genes were shown to be highly inhibited in PCNSL. TGF-β signaling has previously been reported as recurrently inactivated in DLBCL [42] and according to our data is inhibited in PCNSL versus DLBCL pointing to an important role for uncoupling TGF-β signaling in PCNSL. Uncoupling of TGF-β signaling removes its tumor suppressive effect on the malignant B-cells [42]. This implies that inhibitory pharmaceuticals blocking TGF-β, of which multiple are currently in phase 1 clinical trials [43], might not have an effect on the malignant B-cells in PCNSL given expression of the receptor is inhibited. However, the need for PCNSL to inhibit the receptor further highlights the presence and role of TGF-β in the CNS since it is expressed by microglial cells [44]. Interestingly, TGF-β also plays a central role central in creating an immunosuppressive TME [43] and directly inhibits the function of cytotoxic T cells contributing to tumor immune evasion. TGF-β receptor blockers could therefore still play a role in aiding T cell activation despite their likely lack of effect on the malignant cells themselves [45]. Further studies to investigate this are needed, but the RNA expression data highlights how TGF-β signaling is relevant in PCNSL. CIBERSORT analysis was used to identify the immune cell composition based on RNA expression. Results have to be interpreted with some care since the tumor itself is of a immune-cell origin in this study. This most likely explains why the most abundant identified cell types were memory B-cells. Interestingly, RNA expression-based quantification was in line with the CD8 quantification based on IHC and also identified M2-like macrophages as abundant in PNCSL, highlighting the presence of immunosuppressive context.

In conclusion, our findings contribute to the understanding of the complex nature of the TME in PCNSL and multiplex immunohistochemistry has been shown to be an elegant and necessary tool to reach this goal. We show both data in support of immunotherapy, raise some key issues that will need to be addressed and provide a rationale for future (combination) immunotherapy trials.

Acknowledgements Many thanks to Dr. Karen Deraedt, pathologist in ZOL Genk, Belgium, for providing additional clinical follow-up data. MILAN multiplex staining analysis was possible thanks to the expertise of KU Leuven MILAN core facility. This study was supported by grants from KU Leuven (3M040406 and OT14/101), UZ Leuven (RT0817) and the 'Stichting Me To You (www.stichtingmetoyou.be)'. LM is a PhD student, financially supported by KU Leuven (Department of Imaging and Pathology), 'Fonds Vandevordt-Gaul', 'Stefanie's Rozen fonds', 'Fonds Tom Debackere'' and 'Emmanuel van der Schueren fellowship' from 'Kom op tegen Kanker'. TT holds a Mandate for Fundamental and Translational Research from the 'Stichting tegen Kanker' (2014-083 and 2019-091). DD holds the International Roche Chair in hematology, holds a Mandate for Clinical Research from the University Hospitals Leuven and from 'Kom op tegen Kanker' and is a co-founder of 'Stefanie's Rozen Fonds', 'Fonds Tom Debackere voor lymfoomonderzoek' and 'Fonds Jos en Mieke Vandevordt-Gaul voor de pathogenese van zeldzame lymfomen'. GV is founder of the 'Fonds Tom Debackere voor lymfoomonderzoek' and 'Fonds Jos en Mieke Vandevordt-Gaul voor de pathogenese van zeldzame lymfomen' and co-founder of 'Stefanie's Rozen fonds'.

Author contributions Lukas Marcelis [first author]: substantially contributed to manuscript conception, design, acquisition of data and interpretation of results. Asier Antoranz: substantially contributed to data analysis (image analysis). Anne-Marie Delsupehe: substantially contributed to data acquisition (IHC analysis). Pauline Biesemans: substantially contributed to data acquisition (IHC analysis). Julio Finalet Ferreiro: substantially contributed to data analysis (gene expression pathway analysis). Koen Debackere: substantially contributed to manuscript design and data acquisition (clinical data). Peter Vandenberghe: substantially contributed to rewriting and revision of initial manuscript versions. Gregor Verhoef: substantially contributed to rewriting and revision of initial manuscript versions. Olivier Gheysens: substantially contributed to rewriting and revision of initial manuscript versions. Giorgio Cattoretti: substantially contributed to data acquisition and manuscript design (multiplex staining technique). Francesca Maria Bosisio: substantially contributed to data acquisition and manuscript design (multiplex staining technique). Xavier Sagaert: substantially contributed to manuscript conception, design and rewriting. Daan Dierickx: substantially contributed to rewriting and revision of initial manuscript versions and interpretation of clinical data. Thomas Tousseyn [last author]: substantially contributed to manuscript conception, design, acquisition of data, interpretation of results and revision/rewriting of initial manuscript versions.

Compliance with ethical standards

Conflict of interest The authors have no conflicts of interest to declare.

References

1. Kluin PM, Deckert M, Ferry JA (2017) Primary diffuse large B-cell lymphoma of the CNS. In: Swerdlow SH, Campo E, Harris NL, Jaffe ES, Pileri SA (eds) WHO classification of tumours of haematopoietic and lymphoid tissues, revised 4th. IARC, Lyon, pp 300–302
2. Montesinos-Rongen M, Siebert R, Deckert M (2009) Primary lymphoma of the central nervous system: just DLBCL or not? Blood 113:7–10. https://doi.org/10.1182/blood-2008-04-149005
3. Chang C, Lin C-H, Cheng A-L, Medeiros LJ, Chang K-C (2015) Primary central nervous system diffuse large B-cell lymphoma has poorer immune cell infiltration and prognosis than its peripheral counterpart. Histopathology 67:625–635. https://doi.org/10.1111/his.12706
4. Marcelis L, Charlien B, De Zutter A, Biesemans P, Vandenberghe P, Verhoef G, Gheysens O, Sagaert X, Dierickx D, Tousseyn T (2018) Other immunomodulatory/suppressive lymphoproliferative diseases: a single-center series of 72 biopsy confirmed cases. Mod Pathol 31:1457–1469

5. Scott DW, Gascoyne RD (2014) The tumour microenvironment in B cell lymphomas. Nat Rev Cancer 14:517–534. https://doi.org/10.1038/nrc3774
6. Fowler NH, Cheah CY, Gascoyne RD, Gribben J, Neelapu SS, Ghia P, Bollard C, Ansell S, Curran M, Wilson WH, O'Brien S, Grant C, Little R, Zenz T, Nastoupil LJ, Dunleavy K et al (2016) Role of the tumor microenvironment in mature B-cell lymphoid malignancies. Haematologica 101:531–540. https://doi.org/10.3324/haematol.2015.139493
7. Ponzoni M, Berger F, Clement C, Tinguely M, Jouvet A, Ferreri AJM, DellOro S, Terreni MR, Doglioni C, Weis J, Cerati M, Milani M, Iuzzolino P, Motta T, Carbone A, Pedrinis E, Sanchez J, Blay J-Y, Reni M, Conconi A, Bertoni F, Zucca E, Cavalli F, Borisch B, International Extranodal Lymphoma Study Group (2007) Reactive perivascular T-cell infiltrate predicts survival in primary central nervous system B-cell lymphomas. Br J Haematol 138:316–323. https://doi.org/10.1111/j.1365-2141.2007.06661.x
8. Kumari N, Krishnani N, Rawat A, Agarwal V, Lal P (2009) Primary central nervous system lymphoma: prognostication as per international extranodal lymphoma study group score and reactive CD3 collar. J Postgrad Med 55:247–251. https://doi.org/10.4103/0022-3859.58926
9. Komohara Y, Horlad H, Ohnishi K, Ohta K, Makino K, Hondo H, Yamanaka R, Kajiwara K, Saito T, Kuratsu J, Takeya M (2011) M2 macrophage/microglial cells induce activation of Stat3 in primary central nervous system lymphoma. J Clin Exp Hematop 51:93–99
10. He M, Zuo C, Wang J, Liu J, Jiao B, Zheng J, Cai Z (2013) Prognostic significance of the aggregative perivascular growth pattern of tumor cells in primary central nervous system diffuse large B-cell lymphoma. Neuro Oncol 15:727–734. https://doi.org/10.1093/neuonc/not012
11. Four M, Cacheux V, Tempier A, Platero D, Fabbro M, Marin G, Leventoux N, Rigau V, Costes-Martineau V, Szablewski V (2017) PD1 and PDL1 expression in primary central nervous system diffuse large B-cell lymphoma are frequent and expression of PD1 predicts poor survival. Hematol Oncol 35:487–496. https://doi.org/10.1002/hon.2375
12. Sasayama T, Tanaka K, Mizowaki T, Nagashima H, Nakamizo S, Tanaka H, Nishihara M, Mizukawa K, Hirose T, Itoh T, Kohmura E (2016) Tumor-associated macrophages associate with cerebrospinal fluid interleukin-10 and survival in primary central nervous system lymphoma (PCNSL). Brain Pathol 26:479–487. https://doi.org/10.1111/bpa.12318
13. Cho H, Kim S-JSH, Kim S-JSH, Chang JH, Yang WI, Suh C-O, Cheong J-W, Kim YR, Lee JY, Jang JE, Kim YR, Min YH, Kim JS (2017) The prognostic role of CD68 and FoxP3 expression in patients with primary central nervous system lymphoma. Ann Hematol 96:1163–1173. https://doi.org/10.1007/s00277-017-3014-x
14. Cho H, Kim SH, Kim S-J, Chang JH, Yang W-I, Suh C-O, Kim YR, Jang JE, Cheong J-W, Min YH, Kim JS (2017) Programmed cell death 1 expression is associated with inferior survival in patients with primary central nervous system lymphoma. Oncotarget 8:87317–87328. https://doi.org/10.18632/oncotarget.20264
15. Chapuy B, Roemer MGM, Stewart C, Tan Y, Abo RP, Zhang L, Dunford AJ, Meredith DM, Thorner AR, Jordanova ES, Liu G, Feuerhake F, Ducar MD, Illerhaus G, Gusenleitner D, Linden EA, Sun HH, Homer H, Aono M, Pinkus GS, Ligon AH, Ligon KL, Ferry JA, Freeman GJ, van Hummelen P, Golub TR, Getz G, Rodig SJ, de Jong D, Monti S, Shipp MA (2016) Targetable genetic features of primary testicular and primary central nervous system lymphomas. Blood 127:869–881. https://doi.org/10.1182/blood-2015-10-673236
16. Nayak L, Iwamoto FM, LaCasce A, Mukundan S, Roemer MGM, Chapuy B, Armand P, Rodig SJ, Shipp MA (2017) PD-1 blockade with nivolumab in relapsed/refractory primary central nervous system and testicular lymphoma. Blood 129:3071–3073. https://doi.org/10.1182/blood-2017-01-764209
17. Havel JJ, Chowell D, Chan TA (2019) The evolving landscape of biomarkers for checkpoint inhibitor immunotherapy. Nat Rev Cancer 19:133–150. https://doi.org/10.1038/s41568-019-0116-x
18. Chen DS, Mellman I (2017) Elements of cancer immunity and the cancer-immune set point. Nature 541:321–330. https://doi.org/10.1038/nature21349
19. Bosisio FM, Antoranz A, van Herck Y, Bolognesi MM, Marcelis L, Chinello C, Wouters J, Magni F, Alexopoulos L, Stas M, Boecxstaens V, Bechter O, Cattoretti G, van den Oord J (2020) Functional heterogeneity of lymphocytic patterns in primary melanoma dissected through single-cell multiplexing. Elife 9:1–28. https://doi.org/10.7554/elife.53008
20. Miyasato Y, Takashima Y, Takeya H, Yano H, Hayano A, Nakagawa T, Makino K, Takeya M, Yamanaka R, Komohara Y (2018) The expression of PD-1 ligands and IDO1 by macrophage/microglia in primary central nervous system lymphoma. J Clin Exp Hematop 58:95–101. https://doi.org/10.3960/jslrt.18001
21. Illerhaus G, Schorb E, Kasenda B (2018) Novel agents for primary central nervous system lymphoma: evidence and perspectives. Blood 132:681–688. https://doi.org/10.1182/blood-2018-01-791558
22. Bolognesi MM, Manzoni M, Scalia CR, Zannella S, Bosisio FM, Faretta M, Cattoretti G (2017) Multiplex staining by sequential immunostaining and antibody removal on routine tissue sections. J Histochem Cytochem 65:431–444. https://doi.org/10.1369/0022155417719419
23. Cattoretti G, Cattoretti G, Bosisio FM, Marcelis L, Bolognesi MM (2018) Multiple iteractive labeling by antibody neodeposition (MILAN). Protoc Exch. https://doi.org/10.1038/protex.2018.106
24. Morscio J, Dierickx D, Ferreiro JF, Herreman A, Van Loo P, Bittoun E, Verhoef G, Matthys P, Cools J, Wlodarska I, De Wolf-Peeters C, Sagaert X, Tousseyn T (2013) Gene expression profiling reveals clear differences between EBV-positive and EBV-negative posttransplant lymphoproliferative disorders. Am J Transplant 13:1305–1316. https://doi.org/10.1111/ajt.12196
25. Bankhead P, Loughrey MB, Fernández JA, Dombrowski Y, McArt DG, Dunne PD, McQuaid S, Gray RT, Murray LJ, Coleman HG, James JA, Salto-Tellez M, Hamilton PW (2017) QuPath: open source software for digital pathology image analysis. Sci Rep 7:16878. https://doi.org/10.1038/s41598-017-17204-5
26. Blaker YN, Spetalen S, Brodtkorb M, Lingjærde OC, Beiske K, Østenstad B, Sander B, Wahlin BE, Melen CM, Myklebust JH, Holte H, Delabie J, Smeland EB (2016) The tumour microenvironment influences survival and time to transformation in follicular lymphoma in the rituximab era. Br J Haematol 175:102–114. https://doi.org/10.1111/bjh.14201
27. Gomez-Gelvez JC, Salama ME, Perkins SL, Leavitt M, Inamdar KV (2016) Prognostic impact of tumor microenvironment in diffuse large B-cell lymphoma uniformly treated with R-CHOP chemotherapy. Am J Clin Pathol 145:514–523. https://doi.org/10.1093/AJCP/AQW034
28. Camilleri-Broët S, Criniè E, Broët P, Delwail V, Mokhtari K, Moreau A, Kujas M, Raphaël M, Iraqi W, Sautès-Fridman C, Colombat P, Hoang-Xuan K, Martin A (2006) Auniform activated B-cell-like immunophenotype might explain the poor prognosis of primary central nervous system lymphomas: analysis of 83 cases. Blood 107:190–196. https://doi.org/10.1182/blood-2005-03-1024
29. Newman AM, Steen CB, Liu CL, Gentles AJ, Chaudhuri AA, Scherer F, Khodadoust MS, Esfahani MS, Luca BA, Steiner D, Diehn M, Alizadeh AA (2019) Determining cell type abundance and expression from bulk tissues with digital cytometry. Nat Biotechnol 37:773–782. https://doi.org/10.1038/s41587-019-0114-2

30. Marcelis L, Tousseyn T (2019) The tumor microenvironment in post-transplant lymphoproliferative disorders. Cancer Microenviron 12:3–16. https://doi.org/10.1007/s12307-018-00219-5
31. Louveau A, Smirnov I, Keyes TJ, Eccles JD, Rouhani SJ, Peske JD, Derecki NC, Castle D, Mandell JW, Lee KS, Harris TH, Kipnis J (2015) Structural and functional features of central nervous system lymphatic vessels. Nature 523:337–341. https://doi.org/10.1038/nature14432
32. Aspelund A, Antila S, Proulx ST, Karlsen TV, Karaman S, Detmar M, Wiig H, Alitalo K (2015) A dural lymphatic vascular system that drains brain interstitial fluid and macromolecules. J Exp Med 212:991–999. https://doi.org/10.1084/jem.20142290
33. Grywalska E, Pasiarski M, Góźdź S, Roliński J (2018) Immune-checkpoint inhibitors for combating T-cell dysfunction in cancer. Onco Targets Ther 11:6505–6524. https://doi.org/10.2147/OTT.S150817
34. Yi M, Jiao D, Xu H, Liu Q, Zhao W, Han X, Wu K (2018) Biomarkers for predicting efficacy of PD-1/PD-L1 inhibitors. Mol Cancer 17:129. https://doi.org/10.1186/s12943-018-0864-3
35. Gravelle P, Burroni B, Péricart S, Rossi C, Bezombes C, Tosolini M, Damotte D, Brousset P, Fournié J-J, Laurent C (2017) Mechanisms of PD-1/PD-L1 expression and prognostic relevance in non-Hodgkin lymphoma: a summary of immunohistochemical studies. Oncotarget 8:44960–44975. https://doi.org/10.18632/oncotarget.16680
36. Nayyar N, White MD, Gill CM, Lastrapes M, Bertalan M, Kaplan A, D'Andrea MR, Bihun I, Kaneb A, Dietrich J, Ferry JA, Martinez-Lage M, Giobbie-Hurder A, Borger DR, Rodriguez FJ, Frosch MP, Batchelor E, Hoang K, Kuter B, Fortin S, Holdhoff M, Cahill DP, Carter S, Brastianos PK, Batchelor TT (2019) MYD88 L265P mutation and CDKN2A loss are early mutational events in primary central nervous system diffuse large B-cell lymphomas. Blood Adv 3:375–383. https://doi.org/10.1182/bloodadvances.2018027672
37. Ahn E, Araki K, Hashimoto M, Li W, Riley JL, Cheung J, Sharpe AH, Freeman GJ, Irving BA, Ahmed R (2018) Role of PD-1 during effector CD8 T cell differentiation. Proc Natl Acad Sci USA 115:4749–4754. https://doi.org/10.1073/pnas.1718217115
38. Mita Y, Kimura MY, Hayashizaki K, Koyama-Nasu R, Ito T, Motohashi S, Okamoto Y, Nakayama T (2018) Crucial role of CD69 in anti-tumor immunity through regulating the exhaustion of tumor-infiltrating T cells. Int Immunol 30:559–567. https://doi.org/10.1093/intimm/dxy050
39. Kamper P, Bendix K, Hamilton-Dutoit S, Honoré B, Nyengaard JR et al (2011) Tumor-infiltrating macrophages correlate with adverse prognosis and Epstein–Barr virus status in classical Hodgkin's lymphoma. Haematologica 96:269–276. https://doi.org/10.3324/haematol.2010.031542
40. Quaranta V, Schmid MC (2019) Macrophage-mediated subversion of anti-tumour immunity. Cells 8:747. https://doi.org/10.3390/cells8070747
41. He Y, Cao J, Zhao C, Li X, Zhou C, Hirsch FR (2018) TIM-3, a promising target for cancer immunotherapy. Onco Targets Ther 11:7005–7009. https://doi.org/10.2147/OTT.S170385
42. Stelling A, Hashwah H, Bertram K, Manz MG, Tzankov A, Müller A (2018) The tumor suppressive TGF-b/SMAD1/S1PR2 signaling axis is recurrently inactivated in diffuse large B-cell lymphoma. Blood 131:2235–2246. https://doi.org/10.1182/blood-2017-10-810630
43. Batlle E, Massagué J (2019) Transforming growth factor-β signaling in immunity and cancer. Immunity 50:924–940. https://doi.org/10.1016/j.immuni.2019.03.024
44. Zöller T, Schneider A, Kleimeyer C, Masuda T, Potru PS, Pfeifer D, Blank T, Prinz M, Spittau B (2018) Silencing of TGFβ signalling in microglia results in impaired homeostasis. Nat Commun 9:1–13. https://doi.org/10.1038/s41467-018-06224-y
45. Dierickx D, Tousseyn T, Verhoef G, Moyer A (2010) Primary central nervous system post-transplatation lymphoproliferative disorder. Cancer 116:3521. https://doi.org/10.1002/cncr.25340